

# Twisted magnetic structure in ferromagnetic ultrathin Ni films induced by magnetic anisotropy interaction with antiferromagnetic FeMn

Kenta Amemiya,<sup>1,\*</sup> Masako Sakamaki,<sup>1</sup> Mari Mizusawa,<sup>2</sup> and Masayasu Takeda<sup>3</sup>

<sup>1</sup>*Photon Factory and Condensed Matter Research Center, Institute of Materials Structure Science, High Energy Accelerator Research Organization, Tsukuba, Ibaraki 305-0801, Japan*

<sup>2</sup>*Research Center for Neutron Science and Technology, Comprehensive Research Organization for Science and Society, Tokai, Ibaraki 319-1106, Japan*

<sup>3</sup>*Quantum Beam Science Directorate, Japan Atomic Energy Agency, Tokai, Ibaraki 319-1195, Japan*

(Received 5 December 2013; revised manuscript received 23 January 2014; published 5 February 2014)

A twisted magnetic structure in Ni ultrathin films attached to antiferromagnetic FeMn is revealed by a combination of the depth-resolved x-ray magnetic circular dichroism (XMCD) and the polarized neutron reflectivity (PNR) techniques. The depth-resolved XMCD at remanent magnetization shows that the perpendicular magnetization component in the Ni film decreases around the interface to FeMn when the film exhibits perpendicular magnetization, whereas the in-plane component is kept constant through the whole film in the case of in-plane magnetization. Moreover, the PNR data shows that when a weak in-plane magnetic field is applied to a film, which exhibits perpendicular magnetization at the remanent state, an in-plane magnetization component is induced in Ni around the interface to FeMn. These results are reasonably interpreted by assuming that the magnetic moment in the Ni layer is twisted from the perpendicular to the in-plane directions towards the interface to FeMn. Such a magnetic structure is supposed to be induced by a magnetic anisotropy interaction at the interface between ferromagnetic Ni and antiferromagnetic FeMn, which makes the Ni magnetic moment around the interface rotate towards the in-plane direction.

DOI: [10.1103/PhysRevB.89.054404](https://doi.org/10.1103/PhysRevB.89.054404)

PACS number(s): 75.70.-i, 75.25.-j, 75.30.Gw, 78.70.Dm

## I. INTRODUCTION

Among various magnetic interactions between antiferromagnetic (AFM) and ferromagnetic (FM) materials, the magnetic anisotropy interaction has attracted much interest [1,2] because it can be applied to control the magnetic direction of ultrathin films. Wu *et al.* recently reported that the magnetic easy axis of Ni films in FeMn/Ni/Cu(100) bilayers switches from the perpendicular to in-plane directions as the FeMn layer exhibits the AFM state [1]. They attributed the FeMn-induced anisotropy to the interfacial magnetic frustration between Ni and FeMn. The net magnetic moment in each FeMn plane is in the perpendicular direction, and those in adjacent FeMn planes are antiparallel to each other. Therefore when the FeMn/Ni interface has a step structure, the magnetic moments in the Ni layer are parallel or antiparallel to those in the adjacent FeMn plane, depending on the lateral position. This induces a frustration and enhances in-plane magnetization of the FM Ni layer.

So far, a twisted magnetic structure has been suggested in an AFM Co<sub>2</sub>O<sub>3</sub> layer around the interface to a FM Co layer [3]. Similarly, some noncollinear magnetic structure in a FM layer might also be expected when a FM layer undergoes the magnetic anisotropy interaction at the interface to an AFM layer. For instance, if a FM film originally exhibits perpendicular magnetization but the magnetic anisotropy interaction with an AFM layer encourages in-plane magnetization, the spin moment in the FM layer might twist towards the in-plane direction around the interface to the AFM layer, which is similar to the magnetic structure in a domain wall. Direct observation of such noncollinear magnetic structure in

ultrathin films has not been achieved, however, due to a lack of the depth-resolved technique for the magnetic measurement with an atomic-level resolution.

In the present study, we investigate the magnetic depth profile of Ni films in FeMn/Ni/Cu(100) by means of the depth-resolved x-ray magnetic circular dichroism (XMCD) [4–7] and polarized neutron reflectivity (PNR) techniques, and reveal the twisted magnetic structure in the ultrathin Ni layer.

## II. EXPERIMENT

FeMn/Ni/Cu(100) films were grown in an ultrahigh vacuum chamber with a base pressure of  $\sim 1 \times 10^{-7}$  Pa. A 10-mm-diameter Cu(100) single crystal was cleaned by repeated cycles of Ar<sup>+</sup> sputtering at 1.5 keV and subsequent annealing to  $\sim 900$  K. The Ni and FeMn films were then grown on the Cu(100) substrate at room temperature by electron-bombardment evaporation from Ni and Fe rods and from a Mn flake in a Ta crucible. The deposition rate for Fe and Ni was determined before the sample preparation from the oscillatory intensity of a reflection high-energy electron diffraction spot, while that for Mn is estimated by comparing the edge-jump intensities in x-ray absorption spectra at the Fe and Mn *L* edges.

For the XMCD experiment, wedge-shaped Ni films were prepared, and the FeMn layers were homogeneously grown on the Ni films. The XMCD measurement was performed just after the film growth in the same chamber, keeping the vacuum condition. On the other hand, for the PNR measurement, homogeneous films were prepared, which were capped with a 50–100 monolayer (ML) Cu overlayer to protect them from the air. The Cu layer was deposited by the electron-bombardment heating of Cu wires in a Ta crucible.

The XMCD data were recorded at the undulator beamline, BL-16A, at the Photon Factory in Institute of Materials

\*kenta.amemiya@kek.jp

Structure Science, High Energy Accelerator Research Organization, Japan [8–10]. The circularly polarized x rays from the advanced planar polarized light emitted (APPLE)-type undulators were used, and 10-Hz switching between the opposite circular polarizations was also applied. The films were investigated at room temperature by means of the Ni  $L$ -edge depth-resolved XMCD technique, in which the electrons emitted after x-ray absorption were separately collected at different detection angles  $\theta_d$  by using an imaging-type detector consisting of a microchannel plate, a phosphor screen, and a CCD camera. Since the escape depth of the electrons  $\lambda_e$  depends on  $\theta_d$ , a set of XMCD spectra is obtained at different probing depths [4–7]. The partial-electron-yield mode with a retarding voltage of 500 V was adopted so that the Ni  $LMM$  Auger electrons were mainly collected.

Let us discuss what the probing depth means in the depth-resolved XMCD technique. Usually, the number of electrons passing through a solid decays according to an exponential function of the electron path length. In the case that the electrons are emitted along the surface normal direction, the depth  $z$  at which the electrons are generated directly corresponds to the path length, so that the electron decay factor, i.e., the proportion of the electrons which reach the surface, is expressed as  $\exp(-z/\lambda_e)$ . On the other hand, if the electrons are emitted in the grazing direction, the path length to the surface must be longer than  $z$ , and the electrons decay more rapidly as a function of  $z$  compared to the normal emission case. Therefore, in the case of grazing emission, the electron decay factor is also expressed by  $\exp(-z/\lambda_e)$ , but the electron escape depth  $\lambda_e$  is smaller than that for the surface normal emission. Since all the electrons generated at different  $z$  are collected in the XMCD measurement, the observed XMCD data is an average over the depth  $z$ , weighted by a factor of  $\exp(-z/\lambda_e)$ .

The escape depth of the electrons  $\lambda_e$  was experimentally determined at each  $\theta_d$  from the thickness dependence of the edge-jump intensity of the films [4]. The edge-jump intensity does not linearly increase as a function of the film thickness but saturates due to the attenuation of the electrons emitted from inside of the film. Since the degree of the saturation is determined by  $\lambda_e$ , one can estimate  $\lambda_e$  by fitting the thickness dependence of the edge-jump intensity.

The normal and grazing x-ray incidence conditions were adopted to observe the perpendicular and in-plane magnetization components, respectively. The sample was mounted with  $[1\bar{1}0]$  lying in the horizontal plane, and the angle between  $[1\bar{1}0]$  and the x-ray beam was  $30^\circ$  at the grazing incidence condition. A magnetic field of  $\sim 500$ – $2000$  Oe, which was always parallel to the incident x-ray beam, was applied by an electromagnet or a permanent magnet and the magnet was retracted out during the measurements. Thus the remanent magnetization state was investigated. Fe and Mn  $L$ -edge XMCD spectra were also recorded in the total electron yield mode.

To observe the magnetic moment at the buried interface between Ni and FeMn, and to obtain depth-resolved information on the magnetic moment in Ni under a magnetic field, the PNR experiment was carried out at BL-17 in the Materials and Life Science Experimental Facility, Japan Proton Accelerator Research Complex using the pulsed neutron source [11]. We performed the PNR measurements at room temperature at a magnetic field of 1 kOe. The magnetic field and the neutron

polarization were in the in-plane direction of the film. Specular reflectivity curves,  $R^+$  and  $R^-$ , were measured using a  $^3\text{He}$  single neutron detector at glancing angles of 0.3, 0.9, and 2.7 deg to cover a wide wave number ( $q$ ) range. Here,  $R^+$  and  $R^-$  represent the reflectivity when the neutron polarization is parallel and antiparallel to the magnetic field at the sample position, respectively, which were measured without a spin analyzer. The wavelength of the neutron was 0.24–0.64 nm, and the resolution of  $q$  was set to be 10%.

### III. RESULTS AND DISCUSSION

To investigate the changes in magnetic anisotropy of Ni films induced by the interaction with FeMn, the Ni  $L_3$  XMCD intensity at the normal x-ray incidence condition is plotted in Fig. 1 as a function of Ni thickness. Since the data was recorded at the remanent state after magnetizing the film in the perpendicular direction, the XMCD intensity corresponds to the perpendicular magnetization component at the remanent state. The bare Ni film shows the spin reorientation transition (SRT) from the in-plane to perpendicular directions at  $\sim 9$  MLs, which is consistent with the previous report [12,13]. Upon deposition of the 10-ML FeMn film, the perpendicular magnetization region is drastically extended and the critical thickness for the SRT is shifted to  $\sim 6$  MLs. Then the in-plane magnetization region is gradually extended above the FeMn thickness of 10 MLs.

At a glance, this seems to contradict the previous report [1] in which a monotonous increase in the in-plane magnetization region was shown, but this discrepancy comes from the difference in the sample configuration. In the previous report, all films were capped with a Cu overlayer so that the Ni film without FeMn does not correspond to bare Ni but Cu/Ni/Cu(100). Since the Cu overlayer enhances perpendicular magnetization of Ni films [12], the increase in the perpendicular magnetization region found in the present work with  $\sim 10$  ML FeMn could not be observed in the previous study.

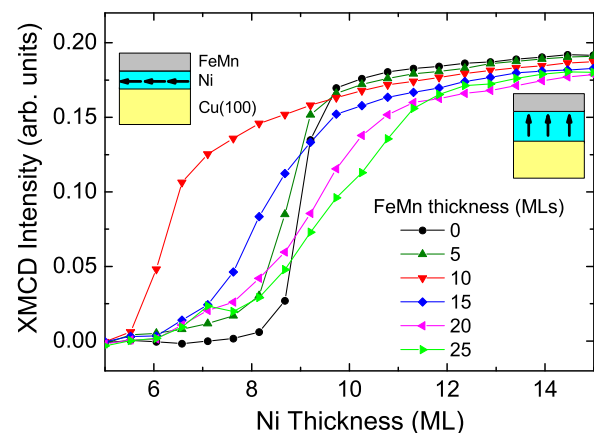


FIG. 1. (Color online) FeMn thickness dependence of Ni  $L_3$  XMCD intensity for FeMn/Ni/Cu(100) as a function of Ni thickness taken in the normal x-ray incidence condition at the remanent magnetization state. The signal intensity corresponds to the perpendicular magnetization component.

First let us discuss the enhancement of perpendicular magnetization of the Ni films induced by  $\sim 10$  ML FeMn. One should remember the fact that the surface of the Ni/Cu(100) films exhibits a large negative magnetic anisotropy energy (MAE), which tends to in-plane magnetization, whereas the inner Ni layers have a positive MAE due to the lattice distortion [12,13]. Therefore perpendicular magnetization is enhanced when the large negative MAE at the surface of Ni is lost by being covered with FeMn. In contrast, the increase in the in-plane magnetization region observed above  $\sim 15$  ML FeMn seems interesting, because it is unlikely that the surface of the Ni films is further affected by such thick FeMn. On the other hand, since the Néel temperature for FeMn is reported to increase with its thickness and to be around room temperature for a 12-ML FeMn film, [14] it seems reasonable to attribute the changes in magnetic anisotropy of the Ni films to the interaction between AFM FeMn and FM Ni, as suggested in the previous report [1].

It is still unclear, however, why magnetic anisotropy is almost unchanged by 5 ML FeMn, though the surface negative MAE of Ni should have been already lost. To discuss this strange behavior, magnetization of the FeMn layer must also be considered. Figure 2 shows Fe and Mn  $L$ -edge XMCD spectra for perpendicularly magnetized FeMn/Ni/Cu(100) films with 5 and 15 ML FeMn, whose Ni thicknesses are 12 and 16 MLs, respectively. One can find a significant XMCD signal for 5 ML FeMn, especially at the Fe edge. In fact, the net magnetic moments in Mn and Fe for 5 ML FeMn are estimated to be  $\sim 0.03$  and  $\sim 0.21 \mu_B/\text{atom}$ , respectively, by applying the sum rules [15,16]. These magnetic moments are considered to be induced by the interaction with the FM Ni layer, though the FeMn layer is basically in the paramagnetic state. Although it is difficult to estimate the MAE of the FeMn layer due to relatively poor data quality at the Fe and Mn edges, we

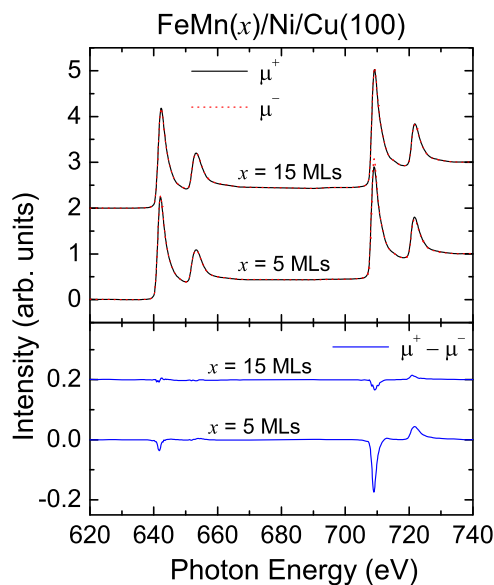


FIG. 2. (Color online) Fe and Mn  $L$ -edge XMCD spectra for FeMn( $x$ )/Ni/Cu(100) taken in the normal x-ray incidence condition. The Ni thicknesses are 12 and 16 MLs for  $x = 5$  and 15 MLs, respectively, and the films show perpendicular magnetization.

speculate that induced magnetization in 5 ML FeMn has a negative MAE, which compensates the loss of the negative MAE at the Ni surface.

On the other hand, the net magnetic moments in Mn and Fe for the 15-ML FeMn layer are estimated to be  $\sim 0.01$  and  $\sim 0.05 \mu_B/\text{atom}$ , respectively. Since the 15-ML FeMn layer is in the AFM state, the observed net magnetic moment is probably attributed to the uncompensated spin at the interface, and its nature must be different from that for the 5-ML FeMn. Therefore the origin of the enhancement of perpendicular magnetization at 10 ML FeMn, as well as that of the increase in the in-plane component above 10 ML, might be also related to the changes in the MAE of FeMn, because the FeMn layer is close to the phase transition at 10 ML. To completely understand the strange behavior in magnetic anisotropy of the FeMn/Ni films, a thorough study, including the depth-resolved observation for the FeMn layer, is necessary.

Hereafter, we concentrate on the changes in the magnetic structure of the Ni films induced by AFM FeMn. Figure 3(a)

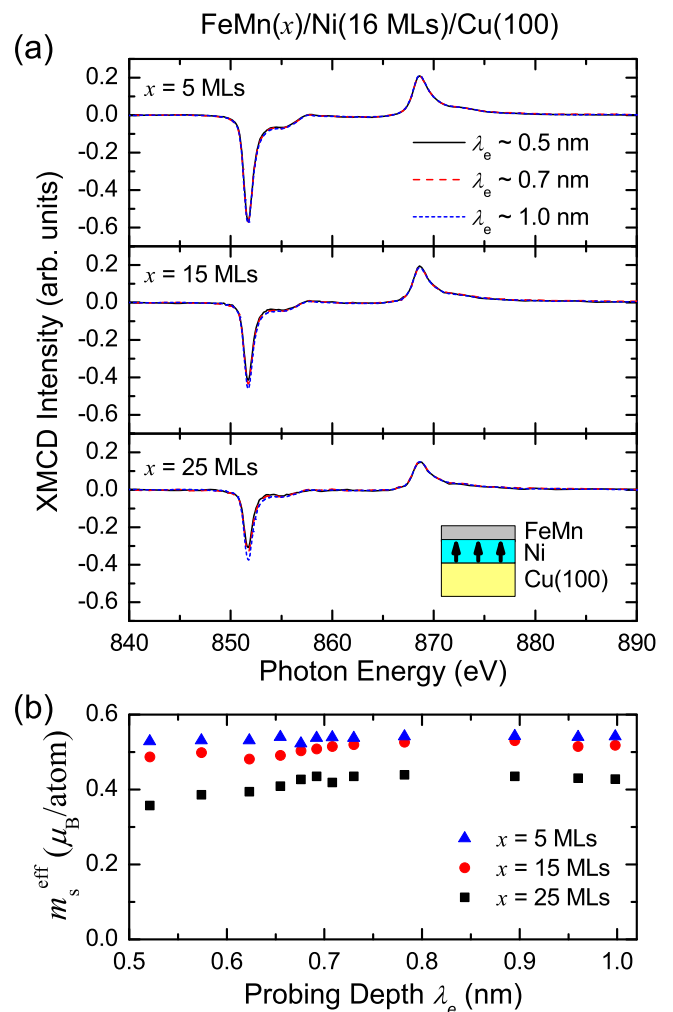


FIG. 3. (Color online) Probing depth ( $\lambda_e$ ) dependence of (a) normal-incidence Ni  $L$ -edge XMCD spectrum and (b) averaged effective spin magnetic moment  $m_s^{\text{eff}}$  estimated by applying the sum rules to each spectrum for FeMn/Ni(16 ML)/Cu(100) with different FeMn thicknesses. The films show perpendicular magnetization.

shows Ni  $L$ -edge depth-resolved XMCD data for perpendicularly magnetized FeMn/Ni(16 ML)/Cu(100) films, taken in the normal incidence condition. With a 5-ML FeMn film, which is still in the paramagnetic state, the XMCD intensity is independent of  $\lambda_e$ , which directly indicates that the Ni film has a uniform magnetization. When the FeMn film starts to exhibit the AFM state at 15 MLs, the XMCD intensity slightly decreases as  $\lambda_e$  decreases, i.e., the surface sensitivity increases, suggesting that the perpendicular magnetization component in Ni decreases around the interface to FeMn. This trend becomes more prominent at 25 ML FeMn, where the FeMn layer is in a strong AFM state.

The perpendicular magnetization component is quantitatively estimated by applying the sum rules [15,16] to the XMCD spectra with different  $\lambda_e$ , and plotted in Fig. 3(b). As described in the previous section, the probing depth  $\lambda_e$  corresponds to the effective escape depth of the emitted electrons. Since the XMCD technique gives us an averaged magnetic moment per atom, the observed magnetic moment is an average over the whole Ni layer weighted by a factor of  $\exp(-z/\lambda_e)$ , where  $z$  represents the depth from the top of the Ni layer. It is thus revealed that the perpendicular magnetization component in the perpendicularly magnetized Ni films decreases around the interface to the FeMn layer when FeMn exhibits the AFM state.

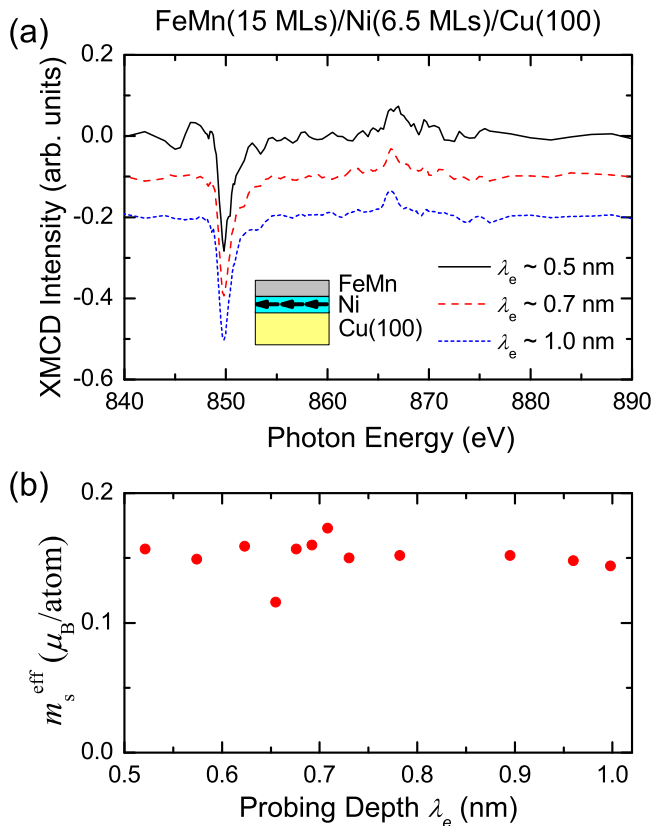


FIG. 4. (Color online) Probing depth ( $\lambda_e$ ) dependence of (a) grazing-incidence Ni  $L$ -edge XMCD spectrum and (b) averaged effective spin magnetic moment  $m_s^{\text{eff}}$ , estimated by applying the sum rules to each spectrum for FeMn(15 ML)/Ni(6.5 ML)/Cu(100). The film shows in-plane magnetization.

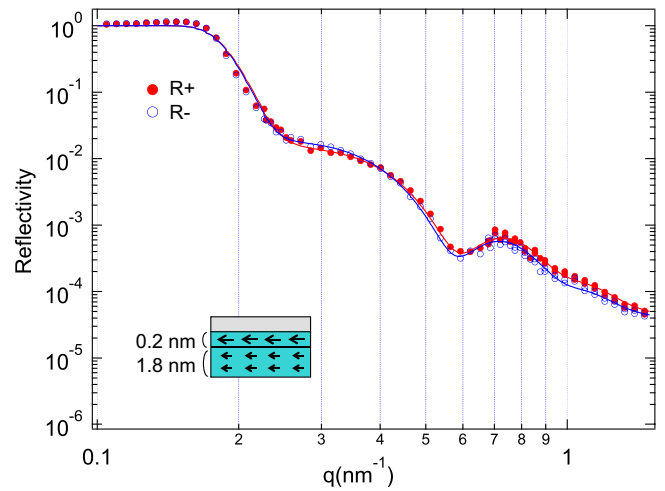


FIG. 5. (Color online) PNR curves,  $R^+$  and  $R^-$ , for Cu(74 ML)/FeMn(21 ML)/Ni(11 ML)/Cu(100) measured at 1 kOe magnetic field. The magnetic field is parallel to the quantization axis of the neutron and is perpendicular to the surface normal direction. The lines are the fit to the data using the magnetic structure model shown in the inset.

Then we investigate the in-plane magnetized sample. Figure 4(a) shows Ni  $L$ -edge depth-resolved XMCD data for an in-plane magnetized FeMn(15 ML)/Ni(6.5 ML)/Cu(100) film, taken in the grazing incidence condition. In contrast to the perpendicularly magnetized films, the XMCD intensity is almost independent of  $\lambda_e$ , though the FeMn layer should exhibit the AFM state at 15 MLs. This discrepancy between the in-plane and perpendicular magnetization leads us to an assumption that the magnetic moment in the Ni films tends to be oriented to the in-plane direction around the interface to FeMn by a magnetic interaction with AFM FeMn. That is, the magnetic moment in the perpendicularly magnetized Ni films might be twisted to the in-plane direction around the interface to AFM FeMn, whereas that in the in-plane magnetized Ni films does not have to rotate because it is already in the in-plane direction.

It is thus suggested that the spin moment in Ni is twisted from the perpendicular to the in-plane directions towards the interface to AFM FeMn. To confirm the twisted magnetic

TABLE I. Structural and magnetic parameters for a Cu/FeMn/Ni/Cu(100) film at the magnetic field of 1 kOe obtained by fitting the PNR curve. SLD represents scattering length density. We adopted a two-region model for the Ni layers, and  $\text{Ni}_{\text{int}}$  and  $\text{Ni}_{\text{inner}}$  represent the interface and inner layer components, respectively.

Layer	SLD ( $\times 10^{10}$ )	Thickness (nm)	Roughness (nm)	Magnetic moment ( $\mu_B/\text{atom}$ )
Cu	6.3	13.3	1.5	(0)
FeMn	3.0	3.8	0.79	(0)
$\text{Ni}_{\text{int}}$	8.5	0.2	0.43	0.32
$\text{Ni}_{\text{inner}}$	8.5	1.8	—	0.20
Cu	(6.5)	(Substrate)	0.50	(0)

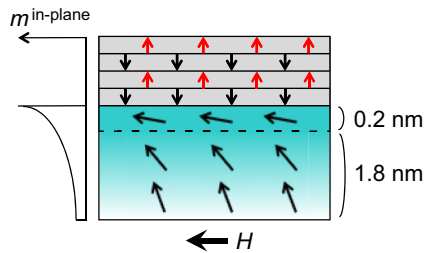


FIG. 6. (Color online) Schematic illustration of magnetic structure at 1 kOe. The Ni magnetic moment gradually rotates from the in-plane to perpendicular directions as approaching the bottom. The in-plane component of the magnetic moment is schematically shown on the left.

structure, we need to detect the in-plane magnetization component in Ni around the interface to FeMn for the perpendicularly magnetized film. It seems difficult to directly observe the canted spin moment by the depth-resolved XMCD technique, however, because the technique can be applied only to the remanent magnetization state. It is likely that the canted spin moments around the interface form some domain structure at the remanent state, resulting in no net in-plane moment. Therefore it is necessary to apply a weak magnetic field along the in-plane direction in order to align the canted spin moments in one direction.

To observe the magnetic depth profile under a magnetic field, we apply the PNR technique to the perpendicularly magnetized FeMn/Ni/Cu(100) film. Please note that the magnetic field and the neutron polarization is in the in-plane direction of the film, whereas the remanent magnetization of Ni is in the perpendicular direction. Therefore, only the in-plane magnetization component induced by the magnetic field is detected. Figure 5 shows the PNR curve at a magnetic field of 1 kOe, which is much smaller than the saturation field,  $\sim 5$  kOe. Two characteristic peaks are observed at  $q = 0.4$  and  $0.75 \text{ nm}^{-1}$ , and there are several intersections between  $R^+$  and  $R^-$ .

We fit the PNR curve by using a two-region model in which the Ni film is separated into two parts, because the interface part is expected to have a different in-plane magnetization component from that in the inner part under a weak magnetic field. Since the net magnetic moment in each FeMn layer aligns in the perpendicular direction [1] and the total magnetic

moment in FeMn vanishes due to the AFM coupling, the magnetic structure of FeMn is not considered in the fitting procedure. We optimize the magnetic moments of the interface and inner parts, as well as the thickness of each part. The obtained structural and magnetic parameters are summarized in Table I. The Ni magnetic moments in the top and bottom parts are  $0.32$  and  $0.20 \mu_B/\text{atom}$ , respectively, which indicates that the magnetic moment in Ni rotates from the perpendicular to the in-plane direction as it approaches the top interface, as depicted in Fig. 6. This model is consistently supported by the above-mentioned depth-resolved XMCD result, and by the assumption that the step-induced magnetic frustration between the AFM FeMn and FM Ni enhances in-plane magnetization in the Ni layer [1].

#### IV. CONCLUSION

We have investigated the magnetic structure around the interface between the FM Ni and AFM FeMn layers by a combination of the depth-resolved XMCD and the PNR techniques. The depth-resolved XMCD at remanent magnetization has shown that the perpendicular magnetization component in the Ni layer decreases around the interface to FeMn when the film exhibits perpendicular magnetization, whereas the in-plane component is kept constant through the whole film in the case of in-plane magnetization. Moreover, the PNR result at a weak (1 kOe) in-plane magnetic field for the FeMn(21 ML)/Ni(11 ML) film, which exhibits perpendicular magnetization at the remanent state, indicates that the in-plane magnetization component in Ni increases around the interface to FeMn. These results consistently suggest a twisted magnetic structure in the ultrathin Ni layer induced by the magnetic anisotropy interaction at the interface between the FM Ni and AFM FeMn layers.

#### ACKNOWLEDGMENTS

The present work has been performed under the approval of the Photon Factory Program Advisory Committee (No. 2010S2-001) and the MLF Program Advisory Committee (No. 2012B140). The authors are grateful for the financial support of the Quantum Beam Technology Program, 2008–2012, from the Ministry of Education, Culture, Sports, Science and Technology (MEXT), Japan.

- [1] J. Wu, J. Choi, A. Scholl, A. Doran, E. Arenholz, C. Hwang, and Z. Q. Qiu, *Phys. Rev. B* **79**, 212411 (2009).
- [2] H. C. Choi, C. Y. You, K. Y. Kim, J. S. Lee, J. H. Shim, and D. H. Kim, *Phys. Rev. B* **81**, 224410 (2010).
- [3] Y. Shiratsuchi, H. Noutomi, H. Oikawa, T. Nakamura, M. Suzuki, T. Fujita, K. Arakawa, Y. Takechi, H. Mori, T. Kinoshita, M. Yamamoto, and R. Nakatani, *Phys. Rev. Lett.* **109**, 077202 (2012).
- [4] K. Amemiya, S. Kitagawa, D. Matsumura, T. Yokoyama, and T. Ohta, *J. Phys.: Condens. Matter* **15**, S561 (2003).
- [5] K. Amemiya, S. Kitagawa, D. Matsumura, T. Ohta, and T. Yokoyama, *Appl. Phys. Lett.* **84**, 936 (2004).
- [6] K. Amemiya, *Phys. Chem. Chem. Phys.* **14**, 10477 (2012).
- [7] M. Sakamaki and K. Amemiya, *Phys. Rev. B* **87**, 014428 (2013).
- [8] K. Amemiya, A. Toyoshima, T. Kikuchi, T. Kosuge, K. Nigorikawa, R. Sumii, and K. Ito, *AIP Conf. Proc.* **1234**, 295 (2010).
- [9] K. Amemiya, M. Sakamaki, T. Koide, K. Ito, K. Tsuchiya, K. Harada, T. Aoto, T. Shioya, T. Obina, S. Yamamoto, and Y. Kobayashi, *J. Phys.: Conf. Ser.* **425**, 152015 (2013).
- [10] K. Tsuchiya, T. Shioya, T. Aoto, K. Harada, T. Obina, M. Sakamaki, and K. Amemiya, *J. Phys.: Conf. Ser.* **425**, 132017 (2013).
- [11] M. Takeda, D. Yamazaki, K. Soyama, R. Maruyama, H. Hayashida, H. Asaoka, T. Yamazaki, M. Kubota, K. Aizawa, M. Arai, Y. Inamura, T. Itoh, K. Kaneko, T. Nakamura, T. Nakatani, K. Oikawa, T. Ohhara, Y. Sakaguchi,

- K. Sakasai, T. Shinohara *et al.*, *Chin. J. Phys.* **50**, 161 (2012).
- [12] W. L. O'Brien, T. Droubay, and B. P. Tonner, *Phys. Rev. B* **54**, 9297 (1996).
- [13] R. Vollmer, Th. Gutjahr-Löser, J. Kirschner, S. van Dijken, and B. Poelsema, *Phys. Rev. B* **60**, 6277 (1999).
- [14] K. Lenz, S. Zander, and W. Kuch, *Phys. Rev. Lett.* **98**, 237201 (2007).
- [15] B. T. Thole, P. Carra, F. Sette, and G. van der Laan, *Phys. Rev. Lett.* **68**, 1943 (1992).
- [16] P. Carra, B. T. Thole, M. Altarelli, and X. Wang, *Phys. Rev. Lett.* **70**, 694 (1993).